JOURNAL OF MATERIALS SCIENCE 27 (1992) 6791–6796

Effect of calcination on characteristics and sintering behaviour of Al_2O_3–ZrO_2 composite powders

CHII-SHYANG HWANG, SHUENN-CHING TSAUR
Department of Materials Engineering, National Cheng-Kung University, Tainan, Taiwan

The effect of calcination on the characteristics and sintering behaviour of zirconia-toughened alumina (ZTA) composite powders has been investigated. TiO_2 was selected as an additive to promote the sinterability of ZTA powders. The starting materials were Al_2O_3 powder, $Zr(OC_3H_7)_4$ and $Ti(OC_3H_7)_4$, and homogeneous ZTA powder containing Zr–O–Ti bonding was prepared. Calcination affected the tetragonal → monoclinic phase transformation temperature of ZrO_2 crystallizing from the gels. Calcination improved the densification rate of ZTA powder compact during sintering, which was attributed to the optimal ZrO_2 particle size and distribution on the surface of alumina. A ZTA specimen with high bulk density and high tetragonal ZrO_2 content was obtained under the conditions of 850 °C/1 h calcination and 1500 °C/1 h sintering.

1. Introduction

The so-called zirconia-toughened alumina (ZTA) ceramics have many applications in which high wear resistance and mechanical strength are required [1–3]. The sintering behaviour and mechanical properties of ZTA ceramics are dependent on ZrO_2 particle distribution, tetragonal ZrO_2 content, aggregates, Al_2O_3 matrix and various additives [4, 5]. The ZrO_2 particle distribution in Al_2O_3 powders was improved by the hydrolysis of Zr alkoxide in an Al_2O_3 slurry [6, 7]. The addition of TiO_2 to ZTA enhanced the densification [8] and maintained the mechanical properties after ageing at high temperature [9]. The authors have prepared ZTA composite powders using commercial Al_2O_3 powders and Zr/Ti alkoxide as starting materials; this method was effective in lowering the sintering temperature [10]. Few studies, however, have focused on the effect of calcination on the densification of ZTA powders prepared through chemical routes. The aim of the present work is to investigate the effect of calcination on the characteristics and the sintering behaviour of ZTA powders, as well as optimizing the calcination conditions for homogeneous ZTA powders.

2. Experimental procedure

2.1. Synthesis of powders

The starting materials were alumina (α-Al_2O_3, 99.99% pure, 0.54 μm average size, Sumitomo Co. AKP-20), zirconium *n*-propoxide ($Zr(OC_3H_7)_4$, Fluka) and tetraisopropyl orthotitanate ($Ti(OC_3H_7)_4$, Tokyo Kasei). Tetraisopropyl orthotitanate was chosen as the source of TiO_2 additive. Al_2O_3 powders were mixed in an ethanol solvent for 10 h, then predetermined amounts of $Zr(OC_3H_7)_4$ and $Ti(OC_3H_7)_4$ were added and mixed for 5 h. The amount of $Zr(OC_3H_7)_4$ and $Ti(OC_3H_7)_4$ was adjusted to obtain 15 mol % ZrO_2 and 2.5 mol % TiO_2. The addition of TiO_2 was below the total solubility limit of ZrO_2 and Al_2O_3. Hydrolysis was induced by adding a 12 M water/ethanol solution. The molar ratio of ZrO_2 and TiO_2 to water was kept constant at 1/24. After the completion of hydrolysis, the solvent was removed by vacuum drying at 40 °C and the powders, which had become ZTA composite powders, were dried at 110 °C. The ZTA powders were then calcined at 450, 650, 850 or 1050 °C for 1 h, and were uniaxially pressed at 25 MPa and isostatically pressed at 98 MPa to obtain rectangular powder compacts of 5 mm × 5 mm × 40 mm.

In order to examine the effect of TiO_2 on the crystallization of zirconia in ZTA powders, pure ZrO_2, TiO_2, co-hydrolysed powders and powder mixture without Al_2O_3 were prepared from $Zr(OC_3H_7)_4$ and/or $Ti(OC_3H_7)_4$ by the same hydrolysis method as that used for synthesizing the ZTA powders. Co-hydrolyzed powder was synthesized by hydrolysing a mixture of $Zr(OC_3H_7)_4$ and $Ti(OC_3H_7)_4$ simultaneously. The powder mixture was formed by the mixing of pure ZrO_2 and TiO_2 powders. The molar ratio of TiO_2/ZrO_2 in the co-hydrolysed powder and powder mixture was 0.143; this ratio was the same in ZTA composite powders.

2.2. Characterization of powders and fired bodies

The green density of powder compact was calculated directly from the dimensions and weight. The powder compacts obtained under different calcination conditions were fired in the furnace of a differential dilatometer (Setaram Co. DHT2050KN), in order to explore the effect of calcination on sintering of these compacts.

0022–2461

Experiments were conducted at 1500 °C for 2 h with heating and cooling rates of 6 °C min^{-1}. Shrinkage of the specimen was monitored continuously throughout sintering. After sintering the final bulk density and dimensions were measured in order to calculate back the instantaneous density and densification rate of specimens. This method was used by Wang and Raj [11] and Tuan and Brook [12]. The density of the sintered specimen was determined by the Archimedes method using water as the immersion medium, and was expressed on a relative scale as the ratio of bulk density to theoretical density of the materials used: 3.987 g cm^{-3} for alumina, 6.05 g cm^{-3} for zirconia and 4.25 g cm^{-3} for titania.

The composition of ZTA powder was determined by X-ray fluorescence analysis. Specific surface area was measured by a multipoint BET method using N_2 gas as the absorbate. The crystalline phases were identified by an X-ray diffractometer (Rigaku Co., 35 kV, 20 mA, time constant 1 s). The X-ray diffraction (XRD) patterns obtained from the as-sintered surface were used to calculate the percentage of tetragonal ZrO_2 (X_t) in each specimen using the equation below [13]:

$$X_t = \frac{I_t(1\,1\,1)}{I_m(1\,1\,\bar{1}) + I_t(1\,1\,1) + I_m(1\,1\,1)} \times 100\%$$

where $I(h\,k\,l)$ = intensity of $(h\,k\,l)$ plane, m = monoclinic phase and t = tetragonal phase.

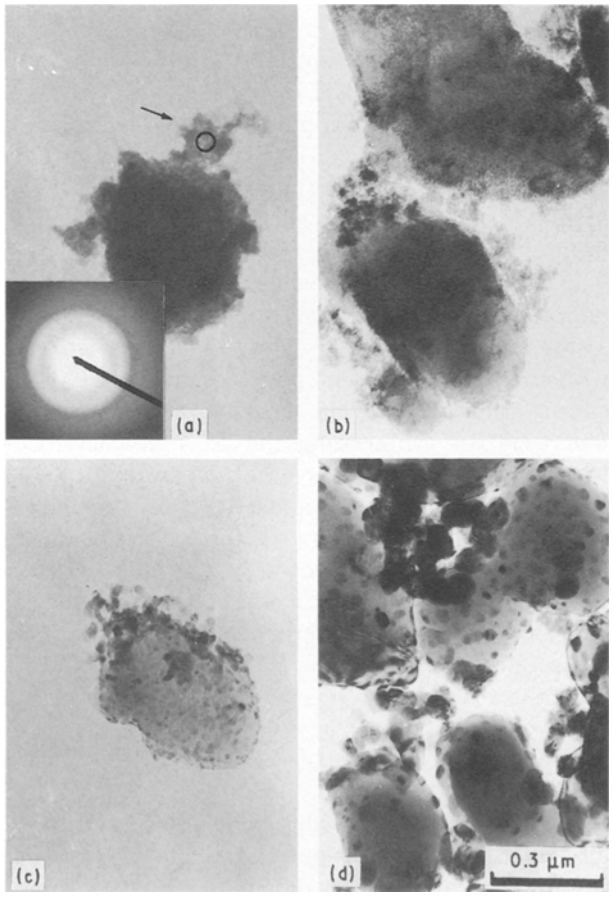

Figure 1 Transmission electron micrographs of Al_2O_3–ZrO_2 composite powder showing bright-field images: (a) dried at 110 °C, and calcined at (b) 450 °C, (c) 850 °C, (d) 1050 °C.

Infrared spectra were obtained (in KBr pellets) using a Hitachi 260-30 i.r. spectrophotometer. Microstructures of the specimens were observed by scanning electron microscopy (Hitachi S-2500) and transmission electron microscopy (TEM, Jeol 400-EX). The average grain sizes of Al_2O_3 and ZrO_2 were estimated by the line-intercept method from SEM pictures.

3. Results and discussion

3.1. Characteristics of the composite powders

X-ray fluorescence analysis reveals that the ZTA composite powders dried at 110 °C contain 15.15 mol % ZrO_2 and 2.39 mol % TiO_2. These values are very close to the predetermined values of 15 and 2.5 mol %. This indicates that the amount of additive can be precisely controlled through the hydrolysis of Zr/Ti alkoxide. A TEM micrograph (Fig. 1a) of the ZTA composite powder dried at 110 °C shows that each individual Al_2O_3 particle has been coated uniformly by hydrolyzed ZrO_2 gels, and the gels are amorphous (indicated by the arrow). After calcination, the ZrO_2 gels have condensed into ultrafine particles and have deposited on to the surface of alumina. The particle size of ZrO_2 in ZTA powders increases with increasing calcination temperature from 450 to 1050 °C (Fig. 1b–d).

Fig. 2 shows the relationship between the specific surface area of ZTA composite powder and calcination temperature. The specific surface area of ZTA powder decreases with increasing calcination temperature, ranging from 66 $m^2 g^{-1}$ (as-dried) to 5.8 $m^2 g^{-1}$ (1050 °C calcination). The lowest value of 5.8 $m^2 g^{-1}$ is still higher than 4.5 $m^2 g^{-1}$ for pure Al_2O_3 powder. It can be concluded that the increase of specific surface area is attributable to the deposition of ZrO_2 fine particles on alumina, which agrees well with the observations from Fig. 1.

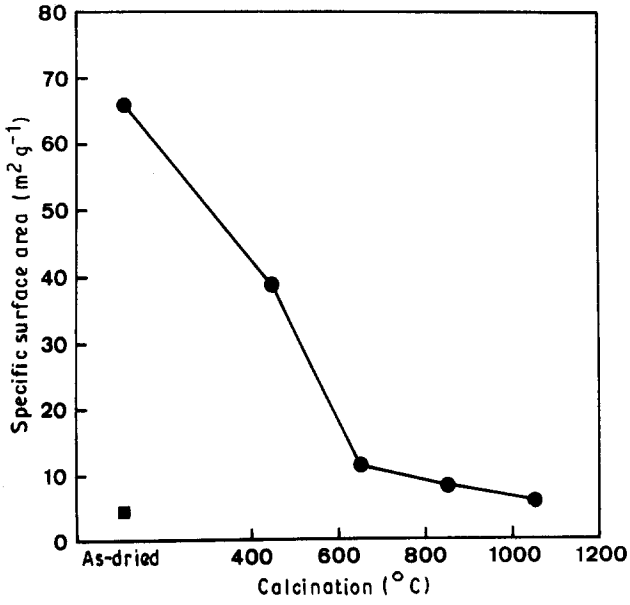

Figure 2 Specific surface area of (●) ZTA powders calcined at various temperatures and (■) Al_2O_3.

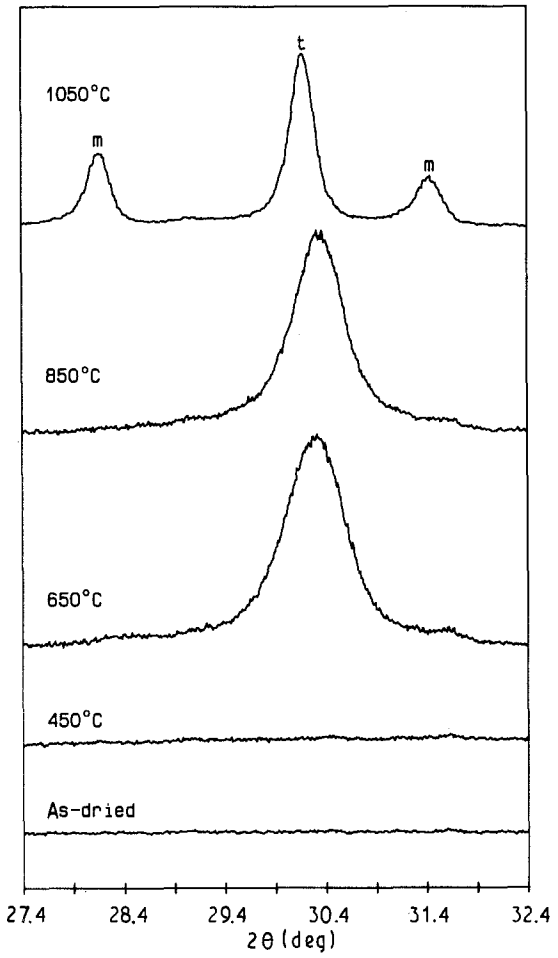

Figure 3 X-ray diffraction patterns of ZTA powders (2.5 mol % TiO_2) dried at 110 °C and calcined at 450–1050 °C.

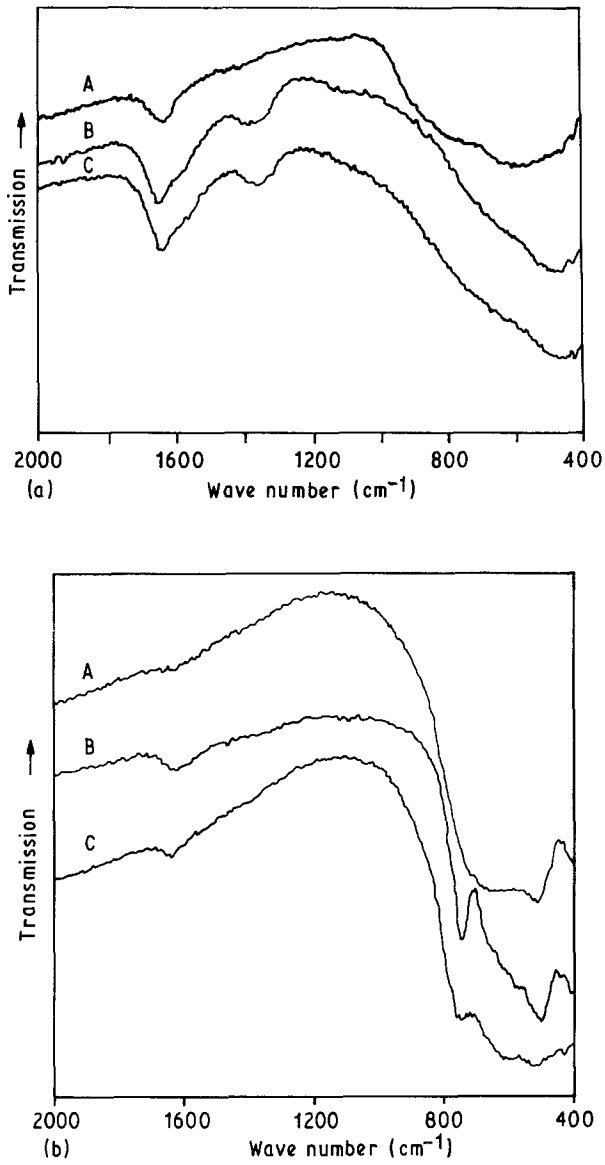

Figure 4 (a) I.r. spectra of (A) pure TiO_2, (B) ZrO_2 and (C) co-hydrolysed ZrO_2–14.3% TiO_2 powders dried at 110 °C. (b) I.r. spectra of (A) pure TiO_2, (B) ZrO_2 and (C) co-hydrolysed ZrO_2–14.3% TiO_2 powders calcined at 850 °C.

XRD results of ZTA composite powders are shown in Fig. 3. Amorphous ZrO_2 in ZTA powder still remains after 450 °C calcination, and only t-ZrO_2 crystallites are found when calcined between 650 and 850 °C. Both t-ZrO_2 and m-ZrO_2 are formed after 1050 °C calcination. For ZTA composite powders without TiO_2, both t-ZrO_2 and m-ZrO_2 are formed after calcination above 450 °C [14]. These various results indicate that the calcination and addition of TiO_2 have a significant influence on the formation of crystalline phases from ZrO_2 gel.

I.r. spectra taken from pure TiO_2, ZrO_2 and co-hydrolysed powders as-dried at 110 °C and subsequently calcined at 850 °C are shown in Fig. 4a and b, respectively. The broad band around 1630 cm^{-1} may result from free water moisture or –OH groups, and that around 1360 cm^{-1} from $-CH_3$ groups [15]. The spectrum of pure TiO_2 powder dried at 110 °C does not show the absorption band at 1360 cm^{-1} (Fig. 4a). It is inferred that the hydrolysis of $Ti(OC_3H_7)_4$ is quite complete as compared with the hydrolysis of pure $Zr(OC_3H_7)_4$ and $Zr/Ti\text{-}(OC_3H_7)_4$. After calcination at 850 °C (Fig. 4b), the disappearance of the 1360 cm^{-1} absorption band is attributed to the burn-out of organic residue. The absorption peak at 510 cm^{-1} from the spectrum of pure TiO_2 powder may be characteristic of Ti–O bonding. Moreover, for pure ZrO_2 powder, the absorption bands at 746, 498, 440 and 410 cm^{-1} may be related to the characteristics of Zr–O bonding [16]. However, the spectrum of co-hydrolysed powder does not show the peaks mentioned above. These results suggest that Zr–O–Ti bonding is formed in the co-hydrolysed powder.

In order to confirm the results of the i.r. spectra the XRD method was employed, and a ZrO_2–14.3 mol % TiO_2 powder mixture was used as a reference. The XRD results for this reference mixture, co-hydrolysed powder and pure TiO_2 powder calcined at 850 °C are shown in Fig. 5. Other than t-ZrO_2 and m-ZrO_2, the anatase and rutile phases of TiO_2 were found from the reference powder. However, neither TiO_2 nor $ZrTiO_4$ phases were found from the XRD pattern of co-hydrolysed powder. It is clear that Zr–O–Ti chemical bonding is formed in the co-hydrolysed powder; therefore, this suggests that the same Zr–O–Ti bonding is formed in the ZTA composite powder. Furthermore, the XRD patterns in Fig. 3 also suggest the same. The

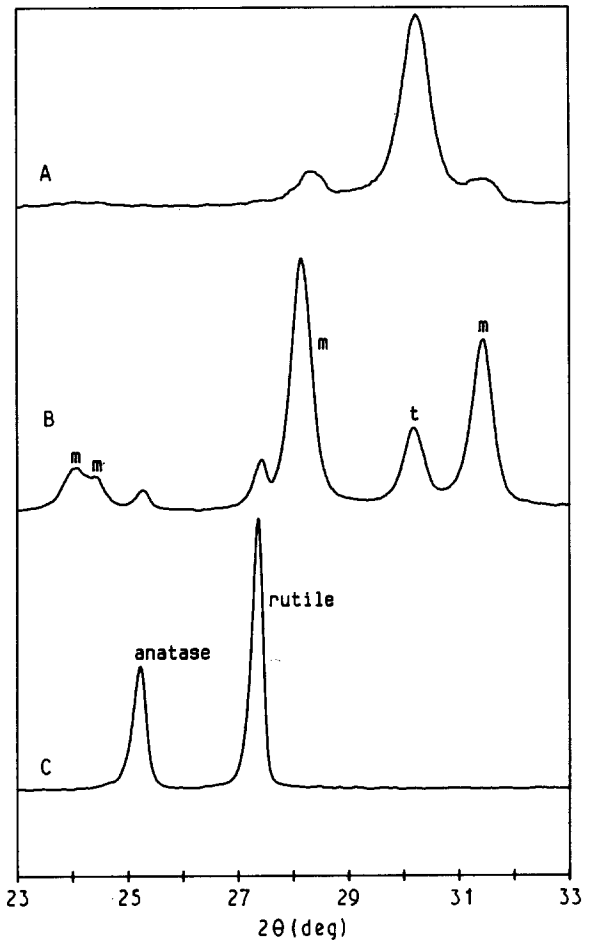

Figure 5 X-ray diffraction patterns of (A) co-hydrolysed ZrO_2–14.3% TiO_2, (B) reference ZrO_2–14.3 mol % TiO_2 and (C) pure TiO_2 powders calcined at 850 °C.

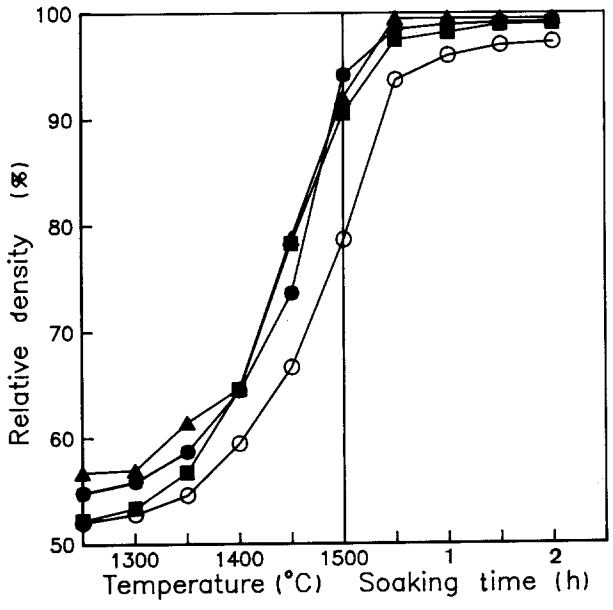

Figure 6 Instantaneous relative densities of ZTA compacts sintering to 1500 °C and soaking 2 h. Calcination: (○) as-dried, (■) 450 °C, (▲) 850 °C, (●) 1050 °C.

above result of Zr–O–Ti bonding agrees well with the XRD results reported by Hirashima *et al.* [17]. In addition, the solubility limit of TiO_2 in ZrO_2 is approximately 16.7 mol % [18], and the dissolution of TiO_2 in ZrO_2 would shift the t → m ZrO_2 phase

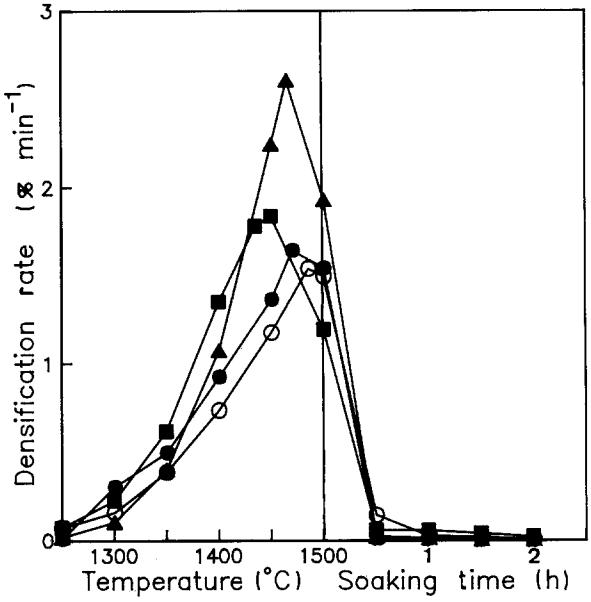

Figure 7 Instantaneous densification rate of ZTA compacts sintering to 1500 °C and soaking 2 h. Calcination: (○) as-dried, (■) 450 °C, (▲) 850 °C, (●) 1050 °C.

transformation temperature [19]. Hence, it is possible that the presence of Zr–O–Ti network structure in the ZTA composite powder leads to the retention of t-ZrO_2, and thus to a shift of the t → m ZrO_2 transformation temperature.

3.2. The densification process

The relative green densities are about 53–56% for all ZTA powder compacts. After sintering, the linear shrinkages in each direction of all compacts are almost the same. This indicates isotropic shrinkage in the densification process. Therefore, the effect of calcination on the instantaneous relative density and densification rate of ZTA powder compacts can be calculated from the linear shrinkage and final bulk density, which is not scattered by the effect of green density. The instantaneous relative density and densification rates of ZTA compacts during sintering to 1500 °C and soaking for 2 h are presented in Figs 6 and 7, respectively. The relative density and densification rate of specimens increase with increasing calcination temperature up to 850 °C. When specimens are heated to 1500 °C, the instantaneous relative density of the specimen calcined at 850 °C is 92%, but only 78% for the specimen without calcination. The densification rate of the specimen calcined at 850 °C can be raised to 2.6% min^{-1} at 1470 °C, but only to about 1.4% min^{-1} for the specimen without calcination. These results show that calcination can improve the sinterability of ZTA powders. Kurita and Hori [3] have reported similar results; when calcining between 800 and 1000 °C, a sintered ZTA specimen in which powders were prepared by the CVD method has a higher relative density.

It is interesting that the specific surface area of as-dried powder is the highest (Fig. 2), but its powder compact has the lowest densification rate. We consider that, before calcination, the fluffy ZrO_2 gel coating on the Al_2O_3 particle surface was thicker, which

would hinder contact between Al_2O_3 particles, and therefore slow down the sintering of ZTA powders. After calcination, the ZrO_2 gel has condensed into round and crystalline particles, whose sizes increase with increasing calcination temperature. The optimal ZrO_2 particle size and distribution obtained by calcination would benefit stacking and sintering of ZTA powders. Therefore, there is an optimal calcination condition for densification of ZTA powder compact, and that is 850 °C for 1 h in this study.

3.3. Microstructures of sintered bodies

Fig. 8 shows SEM pictures of ZTA specimens sintered at 1500 °C for 2 h. For the specimen calcined at 850 °C, the polished surface (Fig. 8a) and thermally etched surface (Fig. 8b) show that pores are almost non-existent and ZrO_2 grains are uniformly dispersed in the Al_2O_3 matrix. For the specimen without calcination (Fig. 8c), void-like pores exist which may be due to burn-out of organic residue or differential sintering of ZrO_2 gel [20]. For the specimen calcined at 1050 °C (Fig. 8d), an abnormal aggregate was observed which may result from excessive calcination. This phenomenon was also observed by Lange *et al.* [20]. The pore and aggregate would inhibit the sintering of ZTA powders. Therefore, as shown in Fig. 7, the specimens without calcination and calcined at 1050 °C have a lower densification rate than the specimen calcined at 850 °C.

The average grain sizes of ZTA sintered specimens are shown in Fig. 9. With increasing calcination temperature, Al_2O_3 and ZrO_2 grain size increased up to 850 °C, then decreased at 1050 °C. The grain size of Al_2O_3 is 1.5–2.0 μm, and 0.6–0.9 μm for ZrO_2. There is not a strong correlation between grain size and calcination temperature for the ZTA specimens.

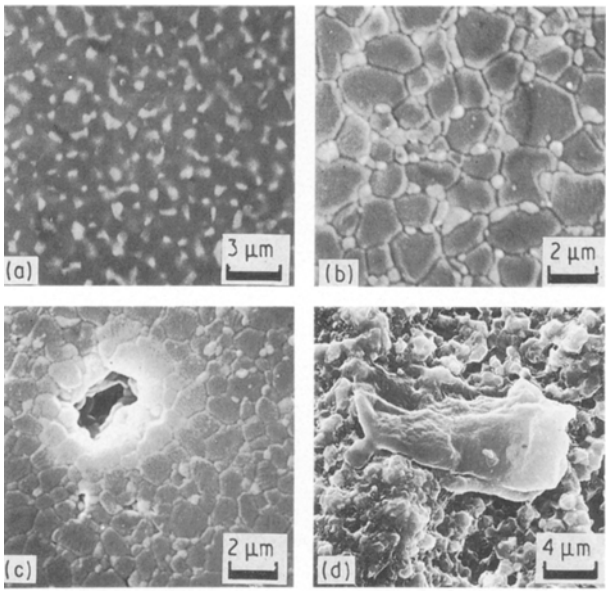

Figure 8 Scanning electron micrographs of ZTA specimens calcined at various temperatures and sintered at 1500 °C for 2 h, showing (a) polished surface, (b) thermally etched surface of specimen calcined at 850 °C, (c) void-like pore of specimen without calcination, and (d) abnormal aggregate of specimen calcined at 1050 °C.

The tetragonal ZrO_2 content (abbreviated X_t) of ZTA sintered specimens as a function of calcination temperature is shown in Fig. 10. The specimen calcined at 850 °C has the highest value of 96%. It is well known that the stability of t-ZrO_2 within an Al_2O_3 matrix depends mainly on the amount of ZrO_2, the constraint of the Al_2O_3 matrix, the shape and location of ZrO_2 grains and the variety of stabilizer. In spite of the few quantitative analyses in this study, it can be inferred that the effect of calcination on the X_t value is related to the distribution of ZrO_2 grains and the constraint of the Al_2O_3 matrix. It is believed that a higher X_t value can improve the toughness of ZTA composite. The effect of calcination on the toughening of ZTA needs to be investigated in the future.

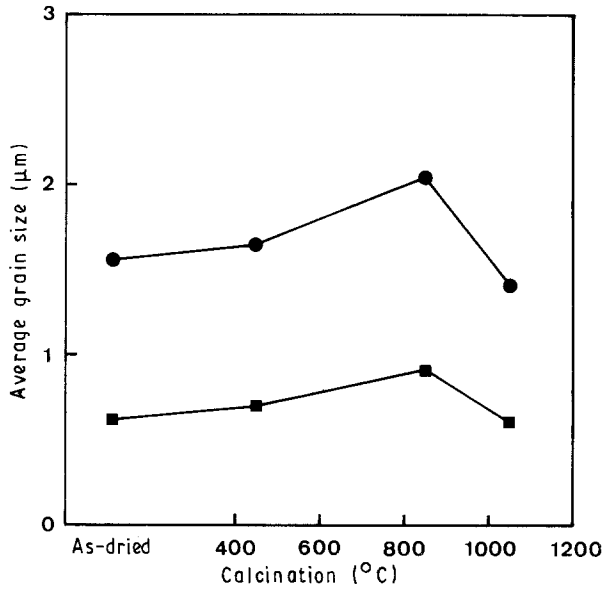

Figure 9 Grain size of (●) Al_2O_3 and (■) ZrO_2 in ZTA sintered specimens for different calcination temperatures.

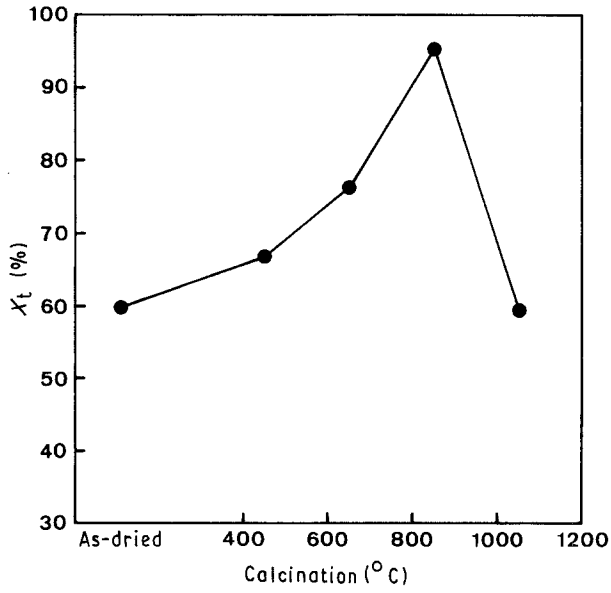

Figure 10 Tetragonal zirconia content of ZTA specimens as a function of calcination temperature.

4. Conclusions

Calcination has a significant effect on the crystalline phase of zirconia in the ZTA composite powder synthesized from Al_2O_3 powder and $Zr/Ti–(OC_3H_7)_4$. Calcination improves the densification rate, the bulk density and the tetragonal ZrO_2 content of ZTA composite. A homogeneous ZTA sintered specimen containing 15 mol % ZrO_2 and 2.5 mol % TiO_2, with relative density >99% and tetragonal ZrO_2 content >90%, can be achieved under the conditions of 850 °C/1 h calcination and 1500 °C/1 h sintering.

Acknowledgement

The authors are grateful to the National Science Council for financial support under contract No. NSC-78-0405-E006-20.

References

1. G. L. MESSING and M. KUMAGAI, *J. Amer. Ceram. Soc.* **72** (1989) 40.
2. N. CLAUSSEN and M. VIIHLE, in "Advances in Ceramics", Vol 3, "Science and Technology of Zirconia I" (American Ceramic Society, Columbus, Ohio (1984) pp. 137–163.
3. R. KURITA and S. HORI, US Patent 4 665 040 (1987).
4. A. H. HEUR, N. CLAUSSEN, W. M. KRIVEN and M. RUHLE, *J. Amer. Ceram. Soc.* **65** (1982) 642.
5. S. R. WITEK and E. P. BUTLER, *ibid.* **69**, (1986) 523.
6. B. FEGLEY Jr, P. WHITE and H. K. BOWEN, *ibid.* **68** (1985) C-60.
7. P. CORTESI and H. K. BOWEN, *Ceram. Internat.* **15** (1989) 173.
8. M. I. OSENDI and J. S. MOYA, *J. Mater. Sci. Lett.* **7** (1988) 15.
9. M. I. OSENDI, B. A. BENDER and D. LEWIS, *Adv. Ceram. Mater.* **3** (1988) 563.
10. C. S. HWANG and W. H. LIN, *Nippon Seramikkusu Kyokai Gakujutsu Ronbunshi* (*J. Ceram. Soc. Jpn*) **99** (1991) 271.
11. J. WANG and R. RAJ, *J. Amer. Ceram. Soc.* **73** (1990) 1172.
12. W. H. TUAN and R. J. BROOK, *J. Mater. Sci.* **24** (1989) 1953.
13. R. C. GRAVIE and P. S. NICHOLSON, *J. Amer. Ceram. Soc.* **54** (1972) 303.
14. C. S. HWANG and S. C. TSAUR, Proceedings of the alumina and aluminium compounds, (Elsevier, 1992).
15. C. J. POUCHERT, "The Aldrich Library of Infrared Spectra", 2nd Edn (Aldrich Chemical Co., Milwaukee, 1978) pp. 1, 63.
16. J. C. DEBSIKDAR, *J. Non-Cryst. Solids* **86** (1986) 231.
17. Y. HIRASHIMA, K. NISHIWAKI, A. MIYAKOSHI, H. TSUIKI, A. UENO and H. NAKABAYASHI, *Bull. Chem. Soc. Jpn* **61** (1988) 1945.
18. M. J. BANNISTER, *J. Amer. Ceram. Soc.* **69** (1986) C-269.
19. F. H. BROWN Jr and P. PUWEZ, *ibid.* **37** (1954) 129.
20. F. F. LANGE, B. I. DAVIS and I. A. AKSAY, *ibid.* **66** (1983) 407.

Received 27 November 1991
and accepted 2 June 1992